

Form and width of spectral line of Josephson Flux-Flow oscillator

Andrey L. Pankratov

Institute for Physics of Microstructures of RAS, Nizhny Novgorod, RUSSIA.

E-mail: alp@ipm.sci-nnov.ru

The behavior of a Josephson flux-flow oscillator in the presence of both bias current and magnetic field fluctuations has been studied. To derive the equation for slow phase dynamics in the limit of small noise intensity the Poincare method has been used. Both the form of spectral line and the linewidth of the flux-flow oscillator have been derived exactly on the basis of technique presented in the book of Malakhov ¹ [1], known limiting cases are considered, limits of their applicability are discussed and appearance of excess noise is explained. Good coincidence of theoretical description with experimental results has been demonstrated.

PACS number(s): 74.50. + r, 74.40. + k

I. INTRODUCTION

Long Josephson oscillators operating in the flux-flow regime [2] are presently considered as possible devices for applications in superconducting millimeter-wave electronics [3]. In comparison to single fluxon oscillators they have higher output power, wider bandwidth, and easier tunability, but they have a wider linewidth [4] of the emitted radiation from the junction. Recent measurements by Koshelets et al. [5,6] have indeed shown a linewidth for a Josephson flux-flow oscillator which is of about one order of magnitude wider than the one derived for a short (lumped) Josephson junction [7–9]. This last property is quite undesirable if one wishes to use such devices, for example, as local oscillators in radioastronomy receivers [3]. For concrete applications it is important to get a model which adequately describes the linewidth of the flux-flow oscillator. With such a model one can hope to control the phenomenon of linewidth broadening by properly choosing the design parameters of the device. A first attempt in this direction was performed by Golubov et al. and Ustinov et al. [10,11] in terms of a particle model for the train of fluxons moving in the junction. However, the authors of [10] calculated the variance of frequency fluctuations (that is quantity difficult to measure) but not a linewidth. Another attempt to derive the linewidth was performed in [12], but the results obtained are restricted by the consideration of "particle-like" picture of fluxon motion in an infinite junction and the linewidth is expressed in quantities that are not easily accessible from experiment in a flux-flow regime, e.g., average interval between fluxons. Besides, magnetic field fluctuations and parametric effects that may lead to additional broadening of the linewidth, were not considered in those papers. Recently, importance of accounting magnetic field fluctuations has been discussed in [13].

The task of deriving of the linewidth of FFO may be decomposed into two parts: one is more experimental and another one is more methodological.

One of the difficulties of the considered problem is absence of understanding of nature of noises of FFO. It is clear, that there are several different noise sources influencing the FFO: natural wideband noises (such as thermal and shot noises), technical narrowband noises and possibly flicker noise. And all these noise sources affect the FFO via fluctuations of both bias current and magnetic field (control line current). Considering present FFO designs [14], one can guess, that there are some noise components in bias and control line currents that are correlated and some that are uncorrelated and lots of detailed experimental study should be performed to understand nature of this complicated mixture of fluctuations.

On the other hand, if we know the parameters of noise (say, parameters of both natural and technical fluctuations), our task is to obtain the linewidth and the form of spectral line of FFO, and on the basis of the obtained characteristics to predict how to improve the noise properties of the oscillator. And here we would like to consider this "methodological" part of the analysis of noise properties of FFO.

The aim of the present paper is to give strictly mathematical derivation of the required fluctuational equation for slow component of the phase that can be done for the most important case of small noise intensity, and present exact derivation of the linewidth and the form of spectral line on the basis of

¹This paper is dedicated to memory of my teacher, The Honored Scientist of Russia, Russian State Prize Winner, Prof. Askold N. Malakhov (5.12.1926-7.11.2000).

methods described in the book by Malakhov [1]. We will assume a certain model of noise sources of FFO bias and control line current fluctuations, as well as we will consider the parametric effect of higher harmonics leading to additional broadening of the spectral line.

II. BASIC EQUATIONS

The electrodynamics of a long Josephson junction in the presence of magnetic field is described by the perturbed sine-Gordon equation

$$\frac{\partial^2 \phi}{\partial t^2} + \alpha \frac{\partial \phi}{\partial t} - \frac{\partial^2 \phi}{\partial x^2} = \eta - \sin(\phi) \quad (1)$$

subject to the boundary conditions

$$\frac{\partial \phi(0, t)}{\partial x} = \frac{\partial \phi(L, t)}{\partial x} = \Gamma. \quad (2)$$

In this equation space and time have been normalized to the Josephson penetration length λ_J and to the inverse plasma frequency ω_p^{-1} , respectively, α is the loss parameter, η is the normalized dc bias current density and Γ is the normalized magnetic field. In accordance with RSJ model [9] one takes the loss parameter $\alpha = \frac{\omega_p}{\omega_c}$, where $\omega_p = \sqrt{2eI_c/\hbar C}$, $\omega_c = 2eI_c R_N/\hbar$, C is the capacitance, R_N is the normal state resistance ($R_N = V/I_{qp}$, V being voltage and I_{qp} – the quasiparticle component of the current), I_c is the critical current, $\eta = J/J_c$ ($I = \int_0^l J(x)dx$, $I_c = \int_0^l J_c(x)dx$, I is the bias current), l is dimensional length of the junction, $L = l/\lambda_J$.

In general, both bias current η and magnetic field Γ (control line current) may fluctuate: $\eta = \eta_0 + \eta_F(x, t)$, $\Gamma = \Gamma_0 + \Gamma_F(x, t)$ and usually these fluctuations are supposed to be wideband noises and are small: for $\eta_0 \neq 0$ and $\Gamma_0 \neq 0$ variances of $\eta_F(x, t)/\eta_0$, $\Gamma_F(x, t)/\Gamma_0$ are much smaller than unity. Therefore, we will consider the noise sources $\eta_F(x, t)$ and $\Gamma_F(x, t)$ as perturbations that do not affect the current-voltage characteristic, but lead to nonzero width of the spectral line. Following [9], we suppose that $\eta_F(x, t)$ is Gaussian noise with zero mean value $\langle \eta_F(x, t) \rangle = 0$ and its spectral density is so wide that $\eta_F(x, t)$ may be treated as white noise with the correlation function:

$$\langle \eta_F(x, t) \eta_F(x', t') \rangle = \frac{2k_B T \omega_p}{R_N I_c J_c \lambda_J} \delta(x - x') \delta(t - t'). \quad (3)$$

Here and in the following $\langle \rangle$ denotes ensemble average, k_B is the Boltzmann constant and T is the temperature. In comparison with [7], we consider simple RSJ model for current fluctuations: usually, at standard working temperature $T = 4.2K$, pair current fluctuations are much smaller than quasiparticle-current fluctuations and may be neglected: $I_p = 0$. Also we do not take into consideration the shot noise contribution that may be neglected if the condition $2k_B T \gg eV$ is fulfilled.

The properties of the magnetic field fluctuations $\Gamma_F(x, t)$ were not studied in the literature. From the present designs of FFO [5,6,14] one can, however, make some conclusions about nature of these fluctuations. In the present layouts the base electrode of the long Josephson junction is employed as a control line. Therefore, wideband bias current fluctuations will enter the control line. Moreover, following recent idea of Koshelets (experimentally confirmed in [13]), even if the control line is isolated from the junction, fluctuating bias current may induce magnetic field, that will affect fluxons. On the other hand, narrowband technical fluctuations also exist there. So, we can model the control line fluctuations as follows: $\Gamma_F(x, t) = \sigma \eta_F(x, t) + \Gamma_I(x, t) + \Gamma_T(x, t)$, where $\Gamma_I(x, t)$ are internal control line pair-current fluctuations (we neglect by $\Gamma_I(x, t) = 0$, supposing that they are much smaller than $\sigma \eta_F(x, t)$) and $\Gamma_T(x, t)$ are narrowband technical fluctuations. Since there are many compensation techniques that allow to significantly eliminate influence of narrowband technical fluctuations [9,5,6,13], we will also neglect them: $\Gamma_T(x, t) = 0$. The question about attenuation factor σ via which bias current fluctuations are converted into magnetic field fluctuations is not trivial and lot of theoretical and especially experimental work should be done to answer this question. It is clear, that σ will be different for different types of FFOs and depends on the junction geometry and distribution of currents in the base electrode. Let us suppose, that the value of σ is known and later we will discuss how σ may be measured. We note, that the approach for linewidth calculation [1] presented below recently was successfully used for calculation of the linewidth of Cherenkov FFO [15]. This approach is rather universal and allows to take into account

almost any noise sources, even flicker noise (for which power spectral density diverges for $\omega \rightarrow 0$, but, nevertheless, calculation of the linewidth may be done in this case [1]) and in the present paper we neglect technical fluctuations only to simplify the analysis.

The flux-flow regime is characterized by excitations which travel on top of a fast rotating background so that the effective nonlinearity in the system is drastically reduced due to fulfilling the following conditions: $\eta/\alpha \gg 1$ and (or) $\Gamma \gg 1$. In order to derive the linearized equation for slow component of the phase $\phi(x, t)$ (that is required for obtaining the spectral characteristics) we will first derive it in the case of zero noise intensity ($\eta_F(x, t) = \Gamma_F(x, t) = 0$) and later will consider noise as small perturbation. In papers [16], [17] linear mode theory and perturbative analysis around rotating background ($\phi = \phi_0 + \psi$, $\psi \ll 1$) have been used to derive the current-voltage characteristic of FFO.

We will use more general Poincare method: obtain the solution as the series with respect to the small parameter $\epsilon = \left(\frac{\alpha}{\eta}\right)^2 \ll 1$. Let us change variables in Eq. (1), $\tau = \frac{\eta}{\alpha}t$, $z = \frac{\eta}{\alpha}x$:

$$\frac{\partial^2 \phi}{\partial \tau^2} + \beta \frac{\partial \phi}{\partial \tau} - \frac{\partial^2 \phi}{\partial z^2} = \beta - \epsilon \sin(\phi), \quad (4)$$

where $\beta = \alpha^2/\eta$.

The steady-state solution of this equation we will find in the form: $\phi(\tau) = \phi_0(\tau) + \epsilon \phi_1(\tau) + \epsilon^2 \phi_2(\tau) + \dots$ ($|\phi_0(\tau)| \gg \epsilon |\phi_1(\tau)| \gg \epsilon^2 |\phi_2(\tau)| \gg \dots$). Substituting this into Eq. (4) we will find the zero order equation:

$$\frac{\partial^2 \phi_0}{\partial \tau^2} + \beta \frac{\partial \phi_0}{\partial \tau} - \frac{\partial^2 \phi_0}{\partial z^2} = \beta. \quad (5)$$

It is easy to see, that the steady-state solution of this equation is: $\phi_0(\tau) = \tau + \gamma z = \frac{\eta}{\alpha}t + \Gamma x$, $\gamma = \alpha\Gamma/\eta$. To get higher order equations we have to decompose $\sin(\phi_0(\tau, z) + \epsilon \phi_1(\tau, z) + \epsilon^2 \phi_2(\tau, z) + \dots)$ into Taylor expansion. From the structure of the considered linear recurrent equations we know, that the steady-state solution $\phi_n(\tau, z)$ may be presented in the form: $\phi_n(\tau, z) = \omega_n \tau + \phi_{np}(\tau, z)$, where $\phi_{np}(\tau, z)$ is periodic nongrowing component.

Let us now collect together all linearly growing components $\omega_n \tau$ and we will get: $\sin(\phi(\tau, z)) = \sin(\{\omega_0 \tau + \epsilon \omega_1 \tau + \epsilon^2 \omega_2 \tau + \dots + \gamma z\} + \epsilon \phi_{1p}(\tau, z) + \epsilon^2 \phi_{2p}(\tau, z) + \dots)$. Now we can linearize $\sin(\phi)$ as: $\sin(\phi) \approx \sin(\omega_J \tau + \gamma z) + \epsilon \phi_{1p}(\tau, z) \cos(\omega_J \tau + \gamma z) + \epsilon^2 \phi_{2p}(\tau, z) \cos(\omega_J \tau + \gamma z) + \dots$, where $\omega_J = \omega_0 + \epsilon \omega_1 + \epsilon^2 \omega_2 + \dots$ is the oscillation frequency ($\omega_0 = 1$), and $\omega_1, \omega_2, \dots, \omega_n, \dots, \phi_{1p}(\tau, z), \phi_{2p}(\tau, z), \dots, \phi_{np}(\tau, z), \dots$ are unknown functions that we want to obtain. Restricting ourselves by consideration the solution up to the 2-nd order only (in principle we can do it up to any order, all equations may be solved recursively), we get the following equations for $\phi_1(\tau, z)$, $\phi_2(\tau, z)$:

$$\frac{\partial^2 \phi_1}{\partial \tau^2} + \beta \frac{\partial \phi_1}{\partial \tau} - \frac{\partial^2 \phi_1}{\partial z^2} = -\sin(\omega_J \tau + \gamma z), \quad (6)$$

$$\frac{\partial^2 \phi_2}{\partial \tau^2} + \beta \frac{\partial \phi_2}{\partial \tau} - \frac{\partial^2 \phi_2}{\partial z^2} = -\phi_{1p}(\tau) \cos(\omega_J \tau + \gamma z). \quad (7)$$

It is easy to see from Eq. (6) that $\omega_1 = 0$ and substituting the solution in the form

$$\phi_{1p}(\tau, z) = \sum_{n=0}^{\infty} [\bar{A}_{1n} \cos(\omega_J \tau) + \bar{B}_{1n} \sin(\omega_J \tau)] \cos(\bar{k}_n z)$$

into (6) one can find \bar{A}_{1n} and \bar{B}_{1n} :

$$\bar{A}_{1n} = (2 - \delta_{0,n}) \frac{\beta \omega_J I_C - (\bar{k}_n^2 - \omega_J^2) I_S}{(\beta \omega_J)^2 + (\bar{k}_n^2 - \omega_J^2)^2}, \quad (8)$$

$$\bar{B}_{1n} = -(2 - \delta_{0,n}) \frac{\beta \omega_J I_S + (\bar{k}_n^2 - \omega_J^2) I_C}{(\beta \omega_J)^2 + (\bar{k}_n^2 - \omega_J^2)^2}, \quad (9)$$

$$I_S = \frac{1}{L} \int_0^{\bar{L}} \sin(\gamma z) \cos(\bar{k}_n z) dz, \quad I_C = \frac{1}{L} \int_0^{\bar{L}} \cos(\gamma z) \cos(\bar{k}_n z) dz, \quad \bar{L} = \frac{\eta}{\alpha} L. \quad (10)$$

Substituting this solution (where $\omega_J = 1 + \epsilon^2\omega_2$) into Eq. (7), we get:

$$\omega_2 = - \sum_{n=0}^{\infty} \frac{2 - \delta_{0,n}}{2} \left[\frac{(1 + \epsilon^2\omega_2)[I_S^2 + I_C^2]}{(\beta(1 + \epsilon^2\omega_2))^2 + [\bar{k}_n^2 - (1 + \epsilon^2\omega_2)^2]^2} \right]. \quad (11)$$

From this equation ω_2 may be found. Analogically to $\phi_{1p}(\tau)$ one can find $\phi_{2p}(\tau)$.

Combining Eqs. (5)-(7) together we can get equation for $\psi(\tau, z) = \phi_0(\tau, z) + \epsilon\phi_1(\tau, z) + \epsilon^2\phi_2(\tau, z) + \dots + \epsilon^n\phi_n(\tau, z)$ that is equivalent to the steady-state case of the original equation (1) up to the n -th order and $\lim_{n \rightarrow \infty} \psi(\tau, z) = \phi(\tau, z)$:

$$\begin{aligned} \frac{\partial^2 \psi}{\partial \tau^2} + \beta \frac{\partial \psi}{\partial \tau} - \frac{\partial^2 \psi}{\partial z^2} = & \beta - \epsilon \sin(\omega_J \tau + \gamma z) - \frac{\epsilon^2}{2L} \int_0^L \sum_{n=0}^{\infty} [\bar{A}_{1n} \cos(\gamma z) - \bar{B}_{1n} \sin(\gamma z)] \cos(\bar{k}_n z) dz - \\ & - \frac{\epsilon^2}{2} \sum_{n=0}^{\infty} [\bar{A}_{1n} \cos(2\omega_J \tau + \gamma z) + \bar{B}_{1n} \sin(2\omega_J \tau + \gamma z)] \cos(\bar{k}_n z) - \dots, \end{aligned} \quad (12)$$

where $\omega_J = 1 + \epsilon\omega_1 + \epsilon^2\omega_2 + \dots + \epsilon^n\omega_n$ is supposed to be known. Here we have presented in the explicit form the term $\phi_{1p}(\tau) \cos(\omega_J \tau + \gamma z)$ and have taken into account that only zero mode term with $m = 0$ will contribute into linearly growing component of $\phi_2(\tau) = \sum_{m=0}^{\infty} \bar{A}_{2m}(\tau) \cos(\bar{k}_m z)$, whereas all contributions

due to $\frac{1}{L} \int_0^L \sum_{n=0}^{\infty} [\bar{A}_{1n} \cos(\gamma z) - \bar{B}_{1n} \sin(\gamma z)] \cos(\bar{k}_n z) \cos(\bar{k}_m z) dz$, $m \neq 0$, will decay with time.

Now, before introducing noise sources, it is convenient to change variables back:

$$\frac{\partial^2 \psi}{\partial t^2} + \alpha \frac{\partial \psi}{\partial t} - \frac{\partial^2 \psi}{\partial x^2} = \eta + \alpha\Omega_2 - f(x, t) - \dots, \quad (13)$$

where $f(x, t) = f_s(x, t) + f_c(x, t)$, $f_s(x, t) = \sin(\Omega_J t + \Gamma x)$, $\eta + \alpha\Omega_2 = \alpha\Omega_J$,

$$f_c(x, t) = \frac{1}{2} \sum_{n=0}^{\infty} [A_{1n} \cos(2\Omega_J t + \Gamma x) + B_{1n} \sin(2\Omega_J t + \Gamma x)] \cos(k_n x), \quad (14)$$

$$\alpha\Omega_2 = \frac{1}{L} \int_0^L \frac{1}{2} \sum_{n=0}^{\infty} [A_{1n} \cos(\Gamma x) - B_{1n} \sin(\Gamma x)] \cos(k_n x) dx, \quad (15)$$

A_{1n} and B_{1n} are:

$$A_{1n} = (2 - \delta_{0,n}) \frac{\alpha\Omega_J I_C - (k_n^2 - \Omega_J^2) I_S}{(\alpha\Omega_J)^2 + (k_n^2 - \Omega_J^2)^2}, \quad (16)$$

$$B_{1n} = -(2 - \delta_{0,n}) \frac{\alpha\Omega_J I_S + (k_n^2 - \Omega_J^2) I_C}{(\alpha\Omega_J)^2 + (k_n^2 - \Omega_J^2)^2}, \quad (17)$$

and $I_C = \frac{\Gamma L \sin(\Gamma L) \cos(\pi n)}{(\Gamma L)^2 - (\pi n)^2}$, $I_S = \frac{\Gamma L (1 - \cos(\Gamma L) \cos(\pi n))}{(\Gamma L)^2 - (\pi n)^2}$, $k_n = \pi n / L$, $\Omega_J = \eta\omega_J / \alpha$ is the oscillation frequency.

Let us focus on the equation for the second-order frequency correction (11), that in original variables, substituting explicit form of I_C and I_S , looks like:

$$\Omega_2 = - \sum_{n=0}^{\infty} \frac{(2 - \delta_{0,n})(\eta/\alpha + \Omega_2)(\Gamma L)^2 [1 - \cos(\Gamma L) \cos(\pi n)]}{[(\eta + \alpha\Omega_2)^2 + (k_n^2 - (\eta/\alpha + \Omega_2)^2)^2][(\Gamma L)^2 - (\pi n)^2]^2}. \quad (18)$$

This transcendental equation may be easily solved and the voltage-current characteristic (IVC) of FFO (due to Josephson relation the voltage is proportional to Ω_J) $\Omega_J = \eta/\alpha + \Omega_2$ may be found, see Fig. 1, where results of computer simulation of Eq. (1) and Eq. (18) are presented for $\alpha = 0.2; 0.5$, $L = 5$, $\Gamma = 3$.

On the other hand, expressing bias current η via Ω_J and Ω_2 we arrive to exactly the same expression for the current-voltage characteristic derived in [16], [17]:

$$\eta = \alpha \Omega_J + \sum_{n=0}^{\infty} \frac{(2 - \delta_{0,n}) \alpha \Omega_J (\Gamma L)^2 [1 - \cos(\Gamma L) \cos(\pi n)]}{[(\alpha \Omega_J)^2 + (k_n^2 - \Omega_J^2)^2][(\Gamma L)^2 - (\pi n)^2]^2}. \quad (19)$$

So, if one needs to obtain the function $\Omega_J(\eta)$, Eq. (19) is more useful. If, however, the function $\Omega_J(\Gamma)$ (voltage versus control line current) is of importance, one can use Eq. (18). When necessary (e.g., when η/α is of the order of unity), one can recourse to the 4-th and higher order approximations and derive *IVC* with the desired precision.

The Eq. (13) is the equation for slow component of the phase in the sense that it is considered in the steady-state limit for $t \rightarrow \infty$. Namely such equation is required to derive different steady-state characteristics, such as correlation functions and spectra. Eq. (13) is linear with respect to $\psi(x, t)$, but nonlinear with respect to η and Γ . Substituting now $\eta = \eta_0 + \eta_F(x, t)$, $\Gamma = \Gamma_0 + \Gamma_F(x, t)$ (in our model $\Gamma_F(x, t) = \sigma \eta_F(x, t)$) and $\psi(x, t) = \psi_0(x, t) + \tilde{\psi}(x, t)$ into (13) and linearizing it with respect to small fluctuations ($f(x, t, \eta, \Gamma) = f(x, t, \eta_0, \Gamma_0) + \frac{\partial f(x, t, \eta, \Gamma_0)}{\partial \eta} \Big|_{\eta=\eta_0} \eta_F(x, t) + \frac{\partial f(x, t, \eta_0, \Gamma)}{\partial \Gamma} \Big|_{\Gamma=\Gamma_0} \Gamma_F(x, t) + \dots$), taking into account that $r_d = \frac{\partial \Omega_J(\eta, \Gamma_0)}{\partial \eta} \Big|_{\eta=\eta_0}$ and $r_d^{CL} = \frac{\partial \Omega_J(\eta_0, \Gamma)}{\partial \Gamma} \Big|_{\Gamma=\Gamma_0}$, we will get the following equation for the correction of the phase due to effect of fluctuations $\tilde{\psi}(x, t)$:

$$\tilde{\psi}_{tt} + \alpha \tilde{\psi}_t - \tilde{\psi}_{xx} = (r_d + \sigma r_d^{CL}) \left[\alpha - \frac{\partial f(x, t)}{\partial \Omega_J} \right] \eta_F(x, t), \quad (20)$$

where r_d and r_d^{CL} are dimensionless dynamical resistances of FFO and control line, respectively. Following [1], the linearization with respect to small fluctuations can be done if in the area of evolution of the fluctuating parameter $\eta = \eta_0 + \eta_F(x, t)$ bifurcation points are not located, that corresponds to the previously assumed condition of the smallness of fluctuations: fluctuations are so small that do not affect current-voltage characteristic and, therefore, do not change qualitative behavior of FFO. Equation (20) is more general than its derivation. In spite it is obtained in the second order approximation, all quantities in rhs of (20) are fundamental and improving the approximation up to higher order will only improve quantitative values of r_d and r_d^{CL} and will add components with $\cos 3\Omega_J t$, $\cos 4\Omega_J t$ and so on into $f(x, t)$. The dynamical resistances are originated from the assumption of small noise: fluctuations feel the system as linear if their variance is small at the scale of nonlinearity and current fluctuations are linearly converted into voltage fluctuations via transfer factor that is the derivative of the current-voltage characteristic at the working point and are not connected with "adiabatic approximation": the noise in rhs of (20) is wideband, but the spectrum of $\tilde{\psi}(x, t)$ depends both on properties of $\eta_F(x, t)$ and the differential operator of the lhs of (20). If we will consider the short junction limit of (20) ($\tilde{\psi}_{xx} = 0$, $r_d^{CL} = 0$), neglect by parametric effects $f(x, t) = 0$ and change variables: $\tilde{v} = \tilde{\psi}_t$, $\tau = \alpha r_d t$, we will get the equation for fluctuational component of voltage \tilde{v} , presented in [9] (Eq. 4.34, page 106).

The solution of Eq. (20) can be expressed as a Fourier serie in space: $\tilde{\psi}(x, t) = \sum_{m=0}^{\infty} A_m(t) \cos(k_m x)$,

where $k_m = \pi m/L$. Substituting this anzats into (20), multiplying by $\cos(k_n x)$ and integrating $\frac{1}{L} \int_0^L$, one can get the following equation for $A_m(t)$:

$$\frac{d^2 A_m}{dt^2} + \alpha \frac{d A_m}{dt} + k_m^2 A_m = \xi_m(t), \quad (21)$$

where $\xi_m(t)$ is the projection of the noise along the k_m mode:

$$\xi_m(t) = \frac{2 - \delta_{0,m}}{L} \int_0^L (r_d + \sigma r_d^{CL}) \left[\alpha - \frac{\partial f(x, t)}{\partial \Omega_J} \right] \eta_F(x, t) \cos(k_m x) dx. \quad (22)$$

Let us analyze correlation and spectral properties of random process $\xi_m(t)$. This is nonstationary process due to periodic time dependence of $f(x, t)$ and its autocorrelation function $\langle \xi_m(t) \xi_m(t + \tau) \rangle$ depends on current time t . Moreover, the product $\frac{\partial f(x, t)}{\partial \Omega_J} \eta_F(x, t)$ formally is a process linearly growing in time and does not belong to neither second nor third kind random processes that complicates the analysis. Here we can use one effective trick: let us analyze statistical properties of the process $\zeta_m(t) =$

$\frac{2-\delta_{0,m}}{L} \int_0^L (r_d + \sigma r_d^{CL}) f(x, t) \eta_F(x, t) \cos(k_m x) dx$ that belongs to the third kind if the stationary process $\eta_F(x, t)$ is white noise and later we will take derivative over Ω_J from the square root of the intensity of the noise $\zeta_m(t)$. Using this procedure we can apply the standard technique [1] and obtain the correlation function of the second kind of the process $\zeta_m(t)$:

$$\Phi_\zeta(\tau) = \lim_{T^* \rightarrow \infty} \frac{1}{2T^*} \int_{-T^*}^{T^*} \langle \zeta_m(t) \zeta_m(t + \tau) \rangle dt, \quad (23)$$

that will lead to stationary delta-correlated process with some intensity, and finally we get the following correlation function for the process $\xi_m(\tau)$:

$$\Phi_{\xi_m}(\tau) = \alpha^2 (r_d + \sigma r_d^{CL})^2 D_m \delta(\tau), \quad (24)$$

where

$$D_m = \frac{2k_B T \omega_p}{R_N I_c^2} (2 - \delta_{0,m}) \{1 + H_m\}, \quad (25)$$

$$H_m = \frac{(2 - \delta_{0,m})}{8\alpha^2} \left[\frac{\partial}{\partial \Omega_J} \sqrt{\frac{1}{L} \int_0^L \left[\left(\sum_{i=0}^{\infty} A_{1n} \cos k_n x \right)^2 + \left(\sum_{i=0}^{\infty} B_{1n} \cos k_n x \right)^2 \right] (\cos k_m x)^2 dx} \right]^2. \quad (26)$$

Let us note, that

$$D_0 = \frac{2k_B T \omega_p}{R_N I_c^2} \{1 + H_0\} \quad (27)$$

for $H_0 = 0$ completely coincides with the dimensionalized noise intensity for a short (lumped) Josephson junction (see [9]). The term H_m comes from down conversion of the 2-nd harmonic due to multiplication of $\cos(2\Omega_J t + \Gamma x)$ and $\sin(2\Omega_J t + \Gamma x)$ by the noise term $\eta_F(x, t)$. This effect, as proven in [1], takes place if the power spectral density of the process $\eta_F(x, t)$ is so wide that significantly different from zero at $2\Omega_J$ and higher. The term describing the effect of the first harmonic $\frac{\partial \sin(\Omega_J t + \Gamma x)}{\partial \Omega_J} \eta_F(x, t)$ will not give any (additional) contribution, since the intensity of the fluctuational process $\mu(t) = \sin(\Omega_J t + \Gamma x) \eta_F(x, t)$, $\Phi_{\mu_m}(\tau) = D_m^* \delta(\tau)/2$ will be constant as function of Ω_J and its derivative over Ω_J will give zero. Therefore, we have classical effect [1] of the additional parametric broadening of the main harmonic at the frequency $\omega = \Omega_J$ due to effect of higher harmonics (at $2\Omega_J$, $3\Omega_J$ and so on).

Since for practical FFOs the second harmonic is rather weak (the output signal is nearly sinusoidal), and since, as it will be demonstrated below, noise components $\xi_m(t)$ with $m \neq 0$ have rather small effect on fluctuational characteristics of FFO, we for simplicity of analysis will neglect the term H_m with $m \neq 0$. For $m = 0$ H_0 takes the form:

$$H_0 = \frac{(\eta - \Omega_J/r_d)^2}{16(\alpha\Omega_J)^3(\eta - \alpha\Omega_J)}. \quad (28)$$

In Fig. 2 we present the plot of the ratio between amplitudes of the second and first harmonics A_2/A_1 (diamonds) and the excess noise H_0 (crosses) as functions of Ω_J using the approximate Eq. (18) for $\alpha = 0.5$, $L = 5$, $\Gamma = 3$. It is seen, that with increase of oscillation frequency Ω_J the second harmonic amplitude becomes smaller than the first one (our approximation works better in high-frequency limit), but slightly increases at Fiske and Eck steps. The same qualitative behavior demonstrates the excess noise intensity H_0 . Unfortunately, the expression (28), in spite of its general form, is of restricted usefulness and may give incorrect results at Fiske steps. This is due to the fact that H_m is derived in the second order approximation only, but it contains the factor $1/r_d$. As it is seen from Fig. 1, at Fiske steps the approximation (18) gives significantly underestimated values of dynamical resistance r_d that leads to overestimated values of H_0 . Contrary, at the Eck step, where approximation (18) and results of computer simulation nearly coincide, Eq. (28) gives adequate description of excess noise term H_0 . In the short junction limit $L \rightarrow 0$ one can get the following approximate expression for the excess noise term:

$$H_{0s} = \frac{(\alpha^2 + 2\Omega_J^2)^2}{8\alpha^2\Omega_J^4(\alpha^2 + \Omega_J^2)^3}. \quad (29)$$

III. FORM AND WIDTH OF SPECTRAL LINE OF FFO

In this section we will consider the influence of noise on broadening of spectral line of the FFO. Following the general setup of the problem [1], we will consider the output signal at the end of the junction in the form: $v(L, t) = \Omega_J + \nu(t) + R_0 \cos(\Omega_J t + \int \nu(t) dt)$, where $\nu(t)$ are frequency fluctuations, and $\int \nu(t) dt$ is supposed to be slow process in comparison with $\cos(\Omega_J t)$ (we do not consider here amplitude fluctuations, $R_0 = \text{const}$, since it is known [1] that they lead only to some noisy pedestal and do not influence the linewidth).

The correlation function of frequency fluctuations may be derived from equation (21) (see, e.g. [18]). Since the slow component of the effective noise $\xi_m(t)$ in (21) is stationary, for $m \neq 0$ we can write the equation for autocorrelation function of $A_m(t)$, $K_{A_m}[\tau] = \langle A_m(t) A_m(t + \tau) \rangle$ which depends only on time difference τ :

$$\frac{d^2 K_{A_m}[\tau]}{d\tau^2} + \alpha \frac{dK_{A_m}[\tau]}{d\tau} + k_m^2 K_{A_m}[\tau] = 0, \quad (30)$$

and should be solved with the following initial conditions:

$$\left. \frac{d^2 K_{A_m}[\tau]}{d\tau^2} \right|_{\tau=0} = -\alpha(r_d + \sigma r_d^{CL})^2 D_m / 2, \quad K_{A_m}[0] = \alpha(r_d + \sigma r_d^{CL})^2 D_m / (2k_m^2).$$

The correlation function of $\tilde{\psi}(L, t)$, $K_\psi[\tau]$, may be expressed as follows:

$$K_\psi[\tau] = \sum_{m=0}^{\infty} K_{A_m}[\tau], \quad (31)$$

since $\cos^2(k_m L) = 1$. By the property of the correlation function, the correlation function of frequency fluctuations $\nu(t) = \frac{d\tilde{\psi}(L, t)}{dt}$, $K_\nu[\tau]$, is the negative second derivative of $K_\psi[\tau]$:

$$K_\nu[\tau] = -\frac{d^2 K_\psi[\tau]}{d\tau^2}. \quad (32)$$

One can see, that for $m = 0$ the correlation function $K_{A_m}[\tau]$ diverges, that reflects the only fact, that for the mode $m = 0$ the process $A_0(t)$ is nonstationary. Namely divergence of $K_\psi[\tau]$ (in our case due to divergence of $K_{A_0}[\tau]$) leads to finite linewidths of oscillators [1]: in the opposite case when $K_\psi[\tau]$ is finite the linewidth will be zero. The divergence of $K_{A_0}[\tau]$ does not lead to any mathematical difficulties since we need to obtain $\langle \dot{A}_0(t) \dot{A}_0(t + \tau) \rangle$ that is finite and may be derived from $K_{A_m}[\tau]$, using (32) and limiting transition for $m \rightarrow 0$.

Finally, one can get the following expression for the correlation function of frequency fluctuations:

$$K_\nu[\tau] = \alpha(r_d + \sigma r_d^{CL})^2 D_0 \times \left\{ \frac{1}{2} e^{-\alpha\tau} + e^{-\alpha\tau/2} \sum_{m=1}^{\infty} \left[\cos(f(\alpha, k_m)\tau) - \frac{\alpha}{2f(\alpha, k_m)} \sin(f(\alpha, k_m)\tau) \right] \right\}, \quad (33)$$

where $f(\alpha, k_m) = f(k_m) = \sqrt{k_m^2 - (\frac{\alpha}{2})^2}$. If $k_m^2 < (\frac{\alpha}{2})^2$, then one has to change sin and cos to the corresponding hyperbolic functions.

For stationary and Gaussian frequency fluctuations (since Eq. (21) is linear with Gaussian noise, the probability distribution of A_m is also Gaussian), the form of spectral line may be written as [1]:

$$W_v(\omega) = \frac{R_0^2}{4\pi} \int_{-\infty}^{+\infty} \exp[-\chi(\tau)] \cos \omega \tau d\tau, \quad (34)$$

where $\chi(\tau)$ is statistical structural function that is nonnegative and even function of τ :

$$\chi(\tau) = \frac{1}{2} \int_{-\tau}^{+\tau} (\tau - |\xi|) K_\nu[\xi] d\xi. \quad (35)$$

Substituting $K_\nu[\tau]$ (33) into (35), we get:

$$\chi(\tau) = \frac{1}{2}(r_d + \sigma r_d^{CL})^2 D_0 \times \left\{ \tau + \frac{e^{-\alpha\tau} - 1}{\alpha} + \frac{\alpha L^2}{3} - e^{-\alpha\tau/2} \sum_{m=1}^{\infty} \frac{2\alpha}{k_m^2} \left[\cos(f(k_m)\tau) + \frac{\alpha \sin(f(k_m)\tau)}{2f(k_m)} \right] \right\}, \quad \tau \geq 0. \quad (36)$$

One can check, that the statistical structural function (36) that we will use for calculation of the linewidth and the form of spectral line is a smooth finite function and the sum in (36) is converging due to the term $1/k_m^2$.

For the case of stationary Gaussian fluctuations of frequency the linewidth is defined in the following way [1]:

$$\Delta\Omega = \frac{\pi}{\int_0^{\infty} \exp[-\chi(\tau)] d\tau}. \quad (37)$$

Substituting the structural function (36) into (37), we get the following final expression for the linewidth:

$$\Delta\Omega = \frac{\pi}{\int_0^{\infty} \exp[-F_1(\tau) - F_2(\tau)] d\tau}, \quad (38)$$

where

$$F_1(\tau) = \frac{1}{2}(r_d + \sigma r_d^{CL})^2 D_0 \left[\tau + \frac{e^{-\alpha\tau} - 1}{\alpha} \right], \quad (39)$$

$$F_2(\tau) = \frac{1}{2}(r_d + \sigma r_d^{CL})^2 D_0 \left[\alpha \frac{L^2}{3} - e^{-\alpha\tau/2} \sum_{m=1}^{\infty} \frac{2\alpha}{k_m^2} \left[\cos(f(k_m)\tau) + \frac{\alpha \sin(f(k_m)\tau)}{2f(k_m)} \right] \right]. \quad (40)$$

In the following we will not recourse to two known limiting cases of very fast and very slow frequency fluctuations (Lorentzian and Gaussian form of the spectral line) but perform the exact analysis of linewidth and spectral form on the basis of expressions (34)-(40).

Let us analyze the linewidth given by expressions (38)-(40). First, consider the case of a short Josephson junction $L \rightarrow 0$, $r_d^{CL} = 0$, neglecting by parametric effects $H_m = 0$. Then the function $F_2(\tau)$ disappears: $F_2(\tau) = 0$. If damping coefficient α is large (but, of course, $\eta/\alpha > 1$), one can neglect the term $(e^{-\alpha\tau} - 1)/\alpha$ in (38),(39) and then well-known expression for the linewidth in Lorentzian approximation may be obtained:

$$\Delta\Omega_s = \frac{\pi}{2} r_d^2 D_0, \quad (41)$$

that in dimensional units looks like:

$$\Delta f_s = \frac{1}{2} \left(\frac{2\pi}{\Phi_0} \right)^2 R_d^2 \frac{k_B T}{R_N}. \quad (42)$$

It should be noted, that this expression is larger than one in [7] by a factor of $\pi/2$ (see formula (12) in [7], we neglected by I_p and $R_N = V_0/I_{qp}$ in their notations). This may be explained by different definitions of the linewidth: we define it as the width of rectangle with the equal square [1], that for Lorentzian form of spectral line should give just by a factor of $\pi/2$ larger value than the definition of the linewidth at $1/2$ level, that was used in [7]. In the following we will present all plots of the linewidth (38)-(40) multiplied by the factor $2/\pi$ for correct comparison with experiment where the linewidth is defined at the level $1/2$.

If, however, damping coefficient α is rather small, there may be significant deviation of the linewidth of a short junction from (41) depending on values of D_0 and r_d (at given D_0 and r_d the linewidth will be smaller), and the use of exact formula (38) for $F_2 = 0$ is necessary.

Now let us consider plots of the exact expression of FFO linewidth (38)-(40) neglecting by magnetic field fluctuations $r_d^{CL} = 0$. Our aim here is to understand how spatial modes with $m \neq 0$ influences the linewidth, i.e. how long junction differs from the short one. The plots of the linewidth versus dynamical resistance are presented in Fig. 3 in dimensional units (MHz vs Ohm) for practical FFO parameters [6]: $L = 76.24$, $\alpha = 0.0074$ ($\alpha L < 1$), $\alpha = 0.04$ ($\alpha L > 1$), $T = 4.2K$, $R_N = 0.04 Ohm$, the dynamical

resistance is: $R_d = 0.01 - 10 \text{ Ohm}$; we neglected by the excess noise term $H_0 = 0$. From Fig. 3 one can see, that below certain threshold curves for $\alpha L < 1$ and $\alpha L > 1$ have the same behavior and coincide with the short junction case (42). Above the threshold that depends on noise intensity (27) one can see the effect of spatial modes: the curves split and the linewidth for $\alpha L > 1$ is greater than for $\alpha L < 1$. With increase of noise intensity the threshold region located for $T = 4.2K$ between $R_d = 0.1 - 1 \text{ Ohm}$ will move to the left. However, it should be noted that practical range of dynamical resistance lies from 0.001 to 0.1 Ohm , where the effect of spatial modes can be neglected that confirms our previous assumption to neglect the excess noise term H_m for $m \neq 0$.

Therefore, it seems that in the practical range of parameters the linewidth of FFO may be well described by the following approximate expression that may be derived from (38)-(40) neglecting by spatial modes with $m \neq 0$ and by the term $(e^{-\alpha\tau} - 1)/\alpha$:

$$\Delta f_{FFO} = \frac{1}{2} \left(\frac{2\pi}{\Phi_0} \right)^2 (R_d + \sigma R_d^{CL})^2 \frac{k_B T}{R_N} (1 + H_0), \quad (43)$$

where H_0 is given by (28). Now let us compare the expression (43) (multiplied by $2/\pi$) with the experimental results [6], see Fig. 4. We again take for simplicity $H_0 = 0$, as before $L = 76.24$, $T = 4.2K$, $R_N = 0.04 \text{ Ohm}$; for $\alpha L < 1$: $\alpha = 0.0074$, for $\alpha L > 1$: $\alpha = 0.04$. In [6] R_d^{CL} has not been explicitly measured and we have used σR_d^{CL} as fitting parameter: putting the noise conversion factor $\sigma = 1$ we have chosen R_d^{CL} to fit experimental results only at one point for $R_d \rightarrow 0$: for $\alpha L < 1$ $R_d^{CL} = 0.006 \text{ Ohm}$ and for $\alpha L > 1$ $R_d^{CL} = 0.04 \text{ Ohm}$. One can see good agreement between expression (43) and the results of experiment. More detailed comparison of expressions (38)-(40) and (43) with experimental results obtained in different layouts, taking into account the excess noise term H_0 will be given elsewhere.

In fact, Fig. 4 and the expression (43) give an idea how the noise conversion factor σ may be measured. If noise intensity is known, setting $R_d \ll R_d^{CL}$ one can get the value $(\sigma R_d^{CL})^2$ from experimentally measured plot of the linewidth. On the other hand, the value R_d^{CL} is independently accessible from experiment.

Let us consider the form of spectral line of the FFO. In general [1], the spectral line consists of narrow and high spectral peak that finite width is originated by frequency fluctuations (nonstationary phase fluctuations) and broad and low pedestal due to amplitude fluctuations. If amplitude and frequency fluctuations are correlated but small, there will be also small asymmetric contributions both into the peak and the pedestal. Since in the frame of the present paper we do not consider amplitude fluctuations, below we will consider the form of spectral peak, that may be derived from (34), substituting statistical structural function (36).

Since in practically interesting range of parameters the linewidth is well described by formula (43), we will also neglect by spatial modes $m \neq 0$ in (36) and by $(e^{-\alpha\tau} - 1)/\alpha$ and will get well-known expression for the Lorentzian form of spectral line:

$$W_v(\omega) = \frac{R_0^2}{4\pi} \frac{2(\Delta f_{FFO}/\pi)}{(\Delta f_{FFO}/\pi)^2 + \omega^2}, \quad (44)$$

the width of this curve at the level 1/2 is given by $2(\Delta f_{FFO}/\pi)$, where Δf_{FFO} is given by (43). In Fig. 5 plots of spectral form, given by (34),(36) (solid lines) and the approximation (44) (dashed lines) are presented. It is seen, that for a small dynamical resistance ($R_d = 0.001 \text{ Ohm}$, that corresponds to plato in Fig. 4) the curves absolutely coincide. With increase of R_d the exact expression slightly deviates from the Lorentzian approximation, but in all practical range of parameters (up to $R_d = 0.1 \text{ Ohm}$), formula (44) gives adequate description of the form of spectral line. For larger R_d and noise intensity, the deviation from Lorentzian form will increase and it is necessary to use expressions (34),(36). Note, that in [12] Lorentzian form of spectral line of FFO was predicted using another approach. Recently, Lorentzian form of spectral line of FFO has been experimentally observed in wide range of parameters both at Fiske and Eck steps [13].

If we would separately consider the case of technical fluctuations (since these fluctuations are slow and narrowband the consideration may be performed in the adiabatic approximation and in this case the effect of additional parametric broadening of the linewidth would not appear due to the fact that the spectrum of technical fluctuations is much more narrow than the basic frequency of the FFO), the form of the spectral line will be Gaussian (for Gaussian distributed technical fluctuations) and the linewidth will be given as $\sqrt{2\pi \langle \nu^2 \rangle}$, where $\langle \nu^2 \rangle$ is variance of frequency fluctuations. It should be noted, that if one wishes to consider the joint effect of natural and technical fluctuations (as they coexist in real life), one can not recourse to the Lorentzian and Gaussian limiting cases, but the calculation of the spectral form should be performed using formula (34).

IV. CONCLUSIONS

The aim of the present paper is to investigate the influence of wideband fluctuations of bias current and magnetic field on dynamics of FFO. We have derived analytical expressions both for the form of spectral line of FFO and its width. For practical range of parameters simple approximate expression of the linewidth, that well fits the experimental results, has been given. The appearance of excess noise (in comparison with the short junction linewidth) has been explained by presence of magnetic field fluctuations and by the so-called parametric broadening of spectral line due to influence of higher harmonics. It has been demonstrated that in the practical range of parameters, in the case when thermal fluctuations dominate, the Lorentzian form of spectral line is realized, while for larger values of dynamical resistance and temperature deviations from Lorentzian form may be observed.

V. ACKNOWLEDGMENTS

The author wishes to thank V. P. Koshelets, V. V. Kurin, N. Likhanov, A. Lukyanov, A. N. Malakhov, J. Mygind, M. Salerno, M. Samuelsen and A. Yulin for helpful discussions and the Dpt. of Physics "E.R.Caianello" of the university of Salerno and personally Prof. Mario Salerno for the offered position where significant part of this work has been done. The work has been supported by the Russian Foundation for Basic Research (Project N 99-02-17544, Project N 00-02-16528 and Project N 00-15-96620), by INFN (Istituto Nazionale di Fisica della Materia) and by the MURST (Ministero dell'Universita' e della Ricerca Scientifica e Tecnologica).

-
- [1] A. N. Malakhov, *Fluctuations in Autooscillating Systems* (Science, Moscow, 1968, in Russian).
 - [2] T. Nagatsuma, K. Enpuku, F. Irie, and K. Yoshida, J. Appl. Phys., **54**, 3302 (1983); **56**, 3284 (1984).
 - [3] V. P. Koshelets and S. V. Shitov, Supercond. Sci. Technol., **13**, R53 (2000).
 - [4] E. Joergensen, V.P. Koshelets, R. Monaco, J. Mygind, M.R. Samuelsen, and M. Salerno, Phys. Rev. Lett., **49**, 1093 (1982).
 - [5] V. P. Koshelets, A. Shchukin, I. L. Lapytskaya, and J. Mygind, Phys. Rev. B, **51**, 6536 (1995).
 - [6] V. P. Koshelets, S. V. Shitov, A. V. Shchukin, L. V. Filippenko, J. Mygind, and A. V. Ustinov, Phys. Rev. B, **56**, 5572 (1997).
 - [7] A. J. Dahm, A. Denestein, D. N. Langenberg, W. H. Parker, D. Rogovin and D. J. Scalapino, Phys. Rev. Lett., **22**, 1416 (1969).
 - [8] A. Barone and G. Paternò, *Physics and Applications of the Josephson Effect* (J. Wiley, New York, 1982).
 - [9] K. K. Likharev, *Dynamics of Josephson Junctions and Circuits* (Gordon and Breach, New York, 1986).
 - [10] A. A. Golubov, B. A. Malomed, and A. V. Ustinov, Phys. Rev. B, **54**, 3047 (1996).
 - [11] A. V. Ustinov, H. Kohlstedt, and P. Henne, Phys. Rev. Lett., **77**, 3617 (1996).
 - [12] A. P. Betenev and V. V. Kurin, Phys. Rev. B, **56**, 7855 (1997).
 - [13] V. P. Koshelets, P. N. Dmitriev, A. B. Ermakov, A. S. Sobolev, A. M. Baryshev, P. R. Wesselius and J. Mygind, "Radiation Linewidth of Flux Flow Oscillators", Extended Abstracts of the 8-th International Superconductive Electronics Conference (ISEC'01), Osaka, Japan, June 2001, in press.
 - [14] V. P. Koshelets and J. Mygind, private communication.
 - [15] A. A. Antonov, A. L. Pankratov, A. V. Yulin and J. Mygind, Phys. Rev. B, **61**, 9809 (2000).
 - [16] M. Cirillo, N. Grønbech-Jensen, M. R. Samuelsen, M. Salerno, G. Verona Rinati, Phys. Rev. B, **58**, 12377 (1998).
 - [17] M. Salerno and M. R. Samuelsen Phys. Rev. B, **59**, 14653 (1999).
 - [18] P. Jung, Physics Reports, **234**, 175 (1993).

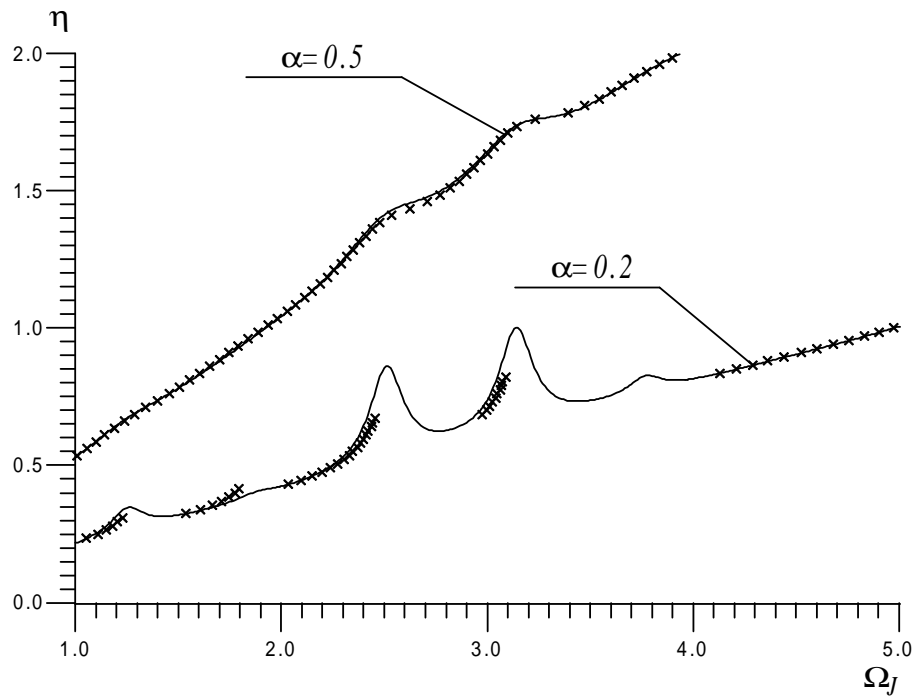


FIG. 1. Current-voltage characteristic. Numerical solution of the sine-Gordon equation is presented by crosses and the second order approximation is given by solid line for $L = 5$, $\Gamma = 3$, $\alpha = 0.2; 0.5$.

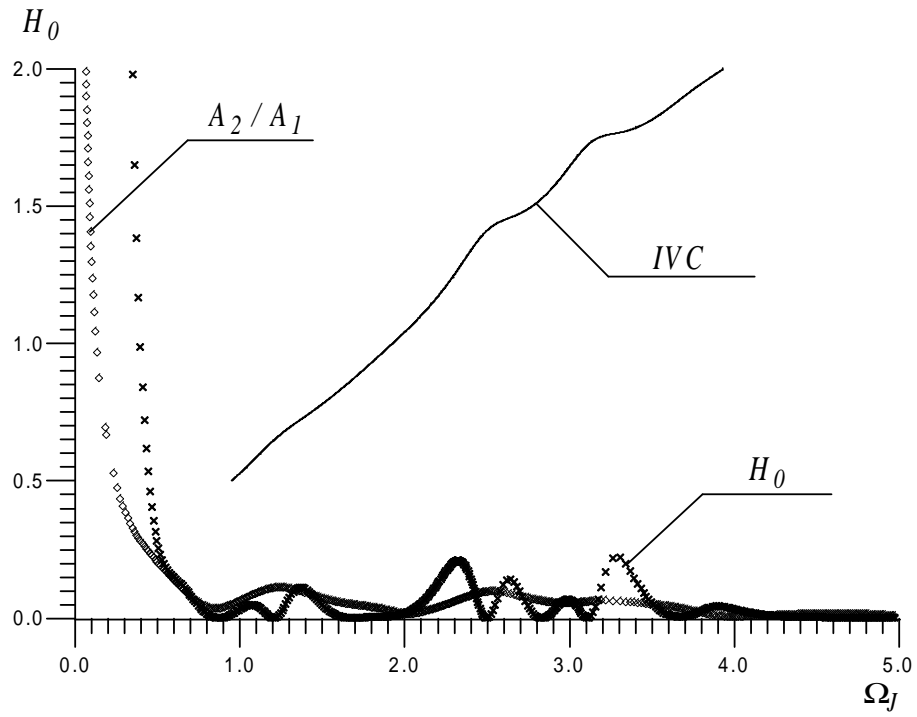


FIG. 2. The excess noise intensity H_0 (crosses) and the ratio between amplitudes of the second and first harmonics A_2/A_1 (diamonds) for $L = 5$, $\Gamma = 3$, $\alpha = 0.5$. For comparison the corresponding current-voltage characteristic (IVC) is given (solid line).

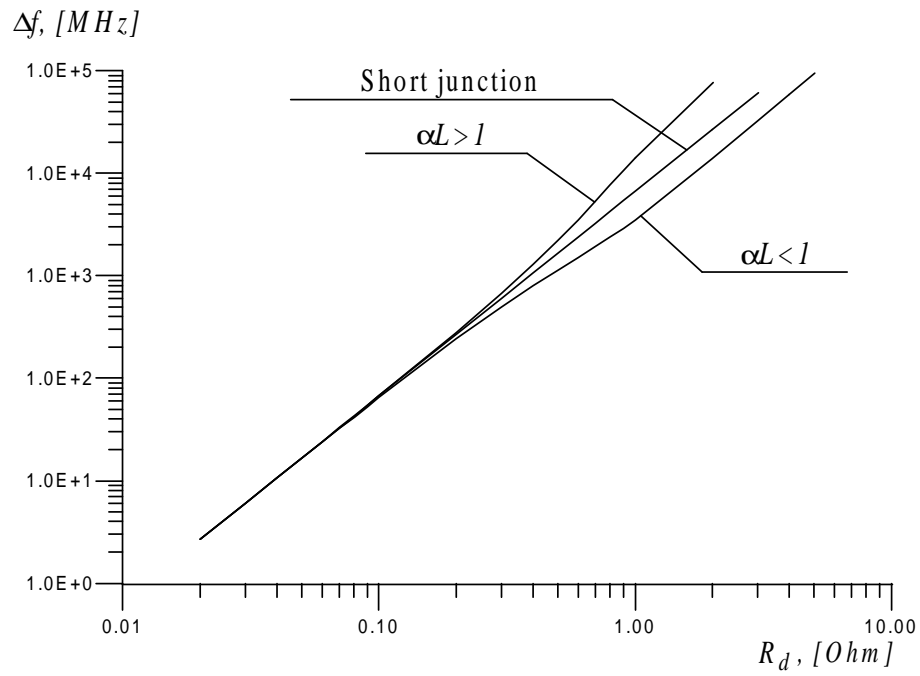


FIG. 3. Illustration of the effect of splitting of the linewidth for $\alpha L < 1$ and $\alpha L > 1$.

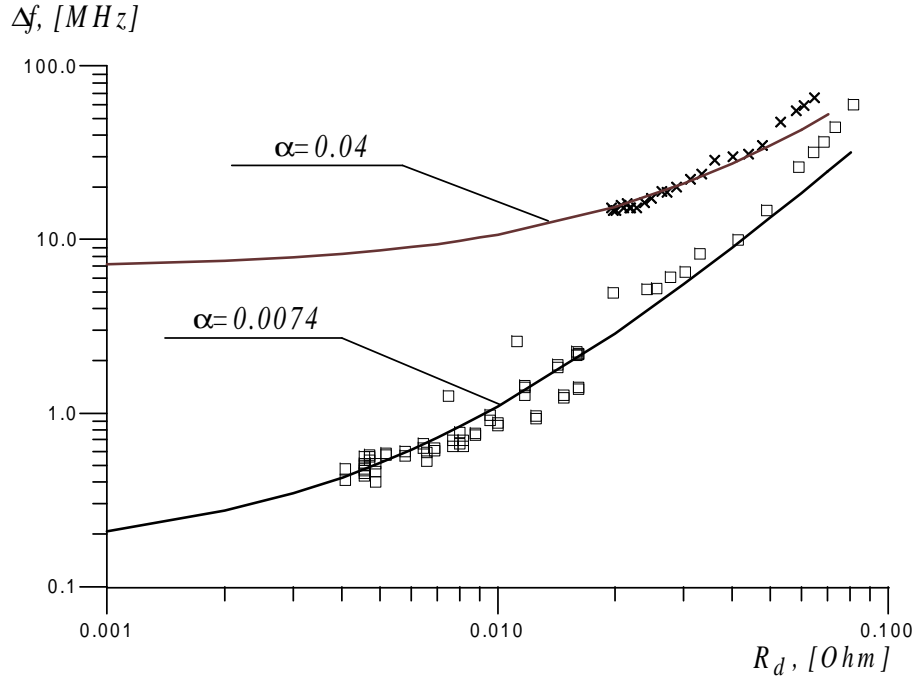


FIG. 4. Comparison of experimental and theoretical linewidths for the parameters: $L = 76.24$, $T = 4.2K$, $R_N = 0.04 \text{ Ohm}$, $\sigma = 1$; for $\alpha L < 1$: $\alpha = 0.0074$, $R_d^{CL} = 0.006 \text{ Ohm}$; for $\alpha L > 1$: $\alpha = 0.04$, $R_d^{CL} = 0.04 \text{ Ohm}$; solid lines - theory, crosses and squares - experimental results.

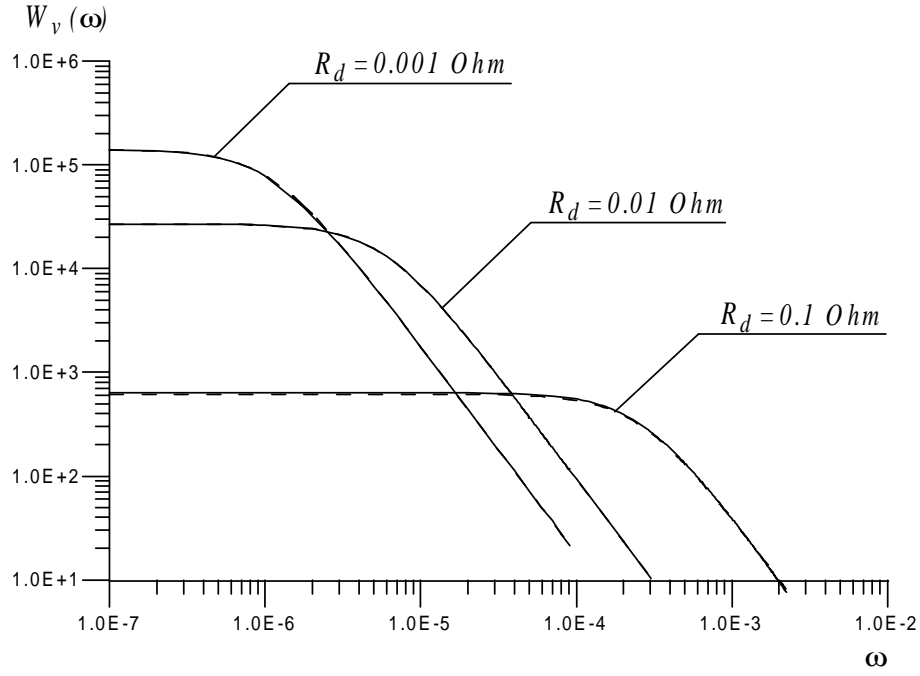


FIG. 5. The form of spectral line: comparison of Lorentzian approximation (dashed lines) and exact expression for the spectral form (solid lines). It is seen, that the corresponding curves coincide.